PROTEIN STRUCTURE REPORTS

THE PROTEIN SOCIETY WILEY

Structure of cytochrome b_5 unique to tardigrades

Yohta Fukuda [ID] | JeeEun Kim | Tsuyoshi Inoue

Graduate School of Pharmaceutical Science, Osaka University, Osaka, Japan

Correspondence
Tsuyoshi Inoue, Graduate School of Pharmaceutical Science, Osaka University, Yamadaoka 1-6, Suita, Osaka, 565-0871, Japan.
Email: t_inoue@phs.osaka-u.ac.jp

Abstract

Cytochrome b_5 is an essential electron transfer protein, which is ubiquitously found in living systems and involved in wide variety of biological processes. Tardigrades (also known as water bears), some of which are famous for desiccation resistance, have many proteins unique to them. Here, we report spectroscopic and structural characterization of a cytochrome b_5 like protein from one of the desiccation-tolerant tardigrades, *Ramazzottius varieornatus* strain YOKOZUNA-1 (RvCytb_5). A 1.4 Å resolution crystal structure revealed that RvCytb_5 is a new cytochrome b_5 protein specific to tardigrades.

KEYWORDS

cytochrome b5, heme, tardigrade, X-ray crystallography

1 | INTRODUCTION

Tardigrades are microscopic multicellular organisms found in almost all environments on Earth from roadside mosses to high mountains and deep sea.[1] Some terrestrial tardigrades can retain their lives under extremely desiccated conditions through transition into a state called anhydrobiosis, in which metabolic processes are undetectable.[2,3] In preparation for anhydrobiosis, the bodies of tardigrades gradually shrink to form a "tun." The tun also shows tolerances to high (151°C)[4] or low (−273°C)[5] temperature, exposure to high energy radiations,[6–8] vacuum,[9,10] high pressure,[11,12] and toxic chemicals.[13,14] Moreover, anhydrobiotic tardigrades are known to survive even in space (low Earth orbit) for 10 days.[15] This extraordinary ability of tardigrades is so famous even in the public that tardigrades appeared in an American famous sci-fi television series Star Trek and a Japanese magical girl animation series Pretty Cure. On the other hand, the detailed molecular basis of tardigrade anhydrobiosis has been largely ambiguous because their key components, tardigrade-specific proteins, are poorly investigated at molecular and atomic levels. To understand structure–function relationships of tardigrade-specific proteins, we have started studies on them

with structural biology approaches.[16–18] In this study, we focus on an electron transfer protein, cytochrome b_5 (Cytb_5), from tardigrades. Electron transfer (ET) plays essential roles in biological processes including photosynthesis and respiration. Cytb_5 mediates many ET reactions relevant to lipid metabolism,[19] steroid synthesis,[20] and methemoglobin reduction.[21] Because Cytb_5 is involved in fundamental biological reactions, it is ubiquitously found in animals, plants, and fungi. Besides, amino acid sequences of Cytb_5 proteins are usually well-conserved. The genome of one of the toughest tardigrades, *Ramazzottius varieornatus* strain YOKOZUNA-1, has several structural genes of Cytb_5 proteins.[22] Judging from their amino acid sequences, most of them closely resemble well-known Cytb_5 proteins; however, one cytochrome b_5 like (Cytb_5-like) protein shows low amino acid sequence similarity to them. Here, we present structural and spectroscopic characterization of this unique Cytb_5-like protein from *R. varieornatus*.

2 | RESULTS AND DISCUSSION

The amino acid sequence of RvCytb_5 shows only 30~36% identity to typical Cytb_5 sequences. In contrast, it shows

slightly higher similarity (39∼46% identity) to that of a protein from a tardigrade *Hypsibius exemplaris* (*He*Cytb_5) and those of some eukaryotic proteins that are annotated as Cytb_5-like proteins but not well characterized (Figure 1a). These Cytb_5-like proteins are phylogenetically distinct from typical Cytb_5 proteins such as mammalian Cytb_5, structures and properties of which are extensively studied (Figure 1b). Cytb_5-like proteins including *Rv*Cytb_5 do not have a C-terminal transmembrane helix, which anchors the proteins on microsomal or mitochondrial membranes; therefore, they are soluble proteins. Tardigrade Cytb_5-like proteins, *Rv*Cytb_5 and *He*Cytb_5, are distinguished from others by insertion of amino acid residues which we named tardigrade specific loop (TS loop) (Figure 1a). *Rv*Cytb_5 has a shorter TS loop than *He*Cytb_5. The TS loops contain Gly, Ser, and Pro residues, which tend to form a disordered region.

UV–visible absorption spectra were measured for *Rv*Cytb_5. The protein at its ferric (Fe^{3+}) form showed a peak corresponding to a Soret band at 412 nm (Figure 1c). The peak corresponding to α and β bands were at 562 (shoulder peak) and 532 nm, respectively. The ferrous (Fe^{2+}) form of *Rv*Cytb_5 exhibited Soret, α, and β band peaks at 422, 558, and 527 nm, respectively. Moreover, it had a weak peak at around 612 nm. These characteristics are similar to known cytochrome b_5,[23] and other bis-histidinyl (i.e., hexacoordinated) globin proteins including neuroglobin[24] and cytoglobin.[25] The ratio of absorption at the β band to that at the trough between the α and β band (A$_{558}$/A$_{540}$) was 2.4 in the ferrous form, indicating a stable hexacoordination state.[26]

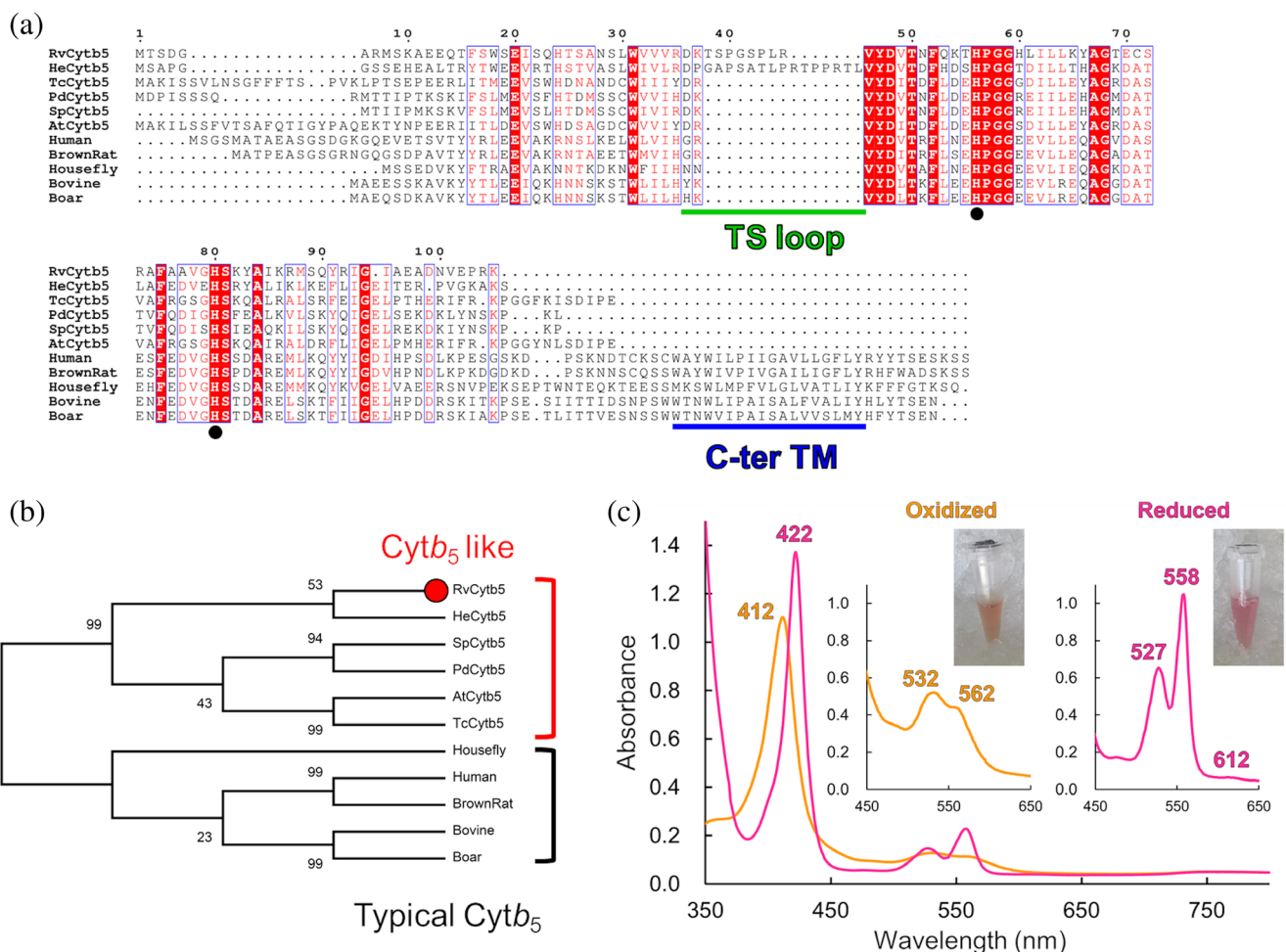The crystal structure was determined at a resolution of 1.4 Å by a single-wavelength anomalous dispersion method

FIGURE 1 Cytochrome b_5 like protein from *Ramazzottius varieornatus* (*Rv*Cytb_5). (a) Amino acid sequence alignment of *Rv*Cytb_5 with similar eukaryotic Cytb_5-like proteins and typical Cytb_5 proteins. Rv: *Ramazzottius varieornatus*; He: *Hypsibius exemplaris* (tardigrade); Tc: *Tribolium castaneum* (insect); Pd: *Pocillopora damicornis* (coral); Sp: *Stylophora pistillata* (coral); At: *Aethina tumida* (insect). Positions of ligand histidine residues are indicated by black circles. (b) Phylogenetic tree for Cytb_5 proteins estimated by a maximum likelihood method. The percentage of trees in which the associated taxa clustered together is shown next to the branches. (c) UV–visible spectra of oxidized (orange) and reduced (pink) *Rv*Cytb_5. Insets show closeup views for the spectra recorded with five times concentrated samples and sample solutions in 1.5 ml micro tubes

TABLE 1 Data collection and refinement statistics

Data collection	
X-ray source	SPring-8 BL44XU
Wavelength (Å)	0.9000
Space group	$P22_12_1$
Unit cell a, b, c (Å)	34.0, 37.5, 77.5
Mosaicity (°)	0.08
Resolution range (Å)	38.8–1.40 (1.42–1.40)[a]
Total no. of reflections/no. of unique reflections	127,971 (6,055)/20,165 (969)
Completeness (%)	99.7 (100)
Redundancy	6.3 (6.2)
$\langle I/\sigma(I)\rangle$	24.0 (3.9)
R_{meas} (all I+ and I−)	0.039 (0.493)
R_{meas} (within I+/I−)	0.038 (0.266)
$CC_{1/2}$	0.999 (0.871)
Overall B factor from Wilson plot (Å^2)	15.5
Refinement	
Resolution range (Å)	38.8–1.40 (1.436–1.400)
Completeness (%)	99.6 (99.9)
No. of reflections, working set	19,138 (1,397)
No. of reflections, test set	985 (69)
R_{work}/R_{free}	0.147/0.171 (0.186/0.204)
No. of non-H atoms	1,017
Protein	791
Ion/ligand	131
Water	95
R.m.s. deviation bonds (Å), angles (°)	0.007, 1.350
Average B factors (Å^2)	28.45
Protein	27.28
Ion/ligand	24.30
Water	43.95
Ramachandran favored/ allowed/disallowed (%)	98.84/1.16/0
PDB code ID	7BWH

[a]Values in parentheses refer to the highest resolution shell.

using a heme iron atom (Fe-SAD) (Table 1). The final R_{work} and R_{free} values are 0.147 and 0.171, respectively. The overall structure of RvCytb_5 is composed of five α helices and five β strands (Figure 2a), which is similar to known Cytb_5 structures such as human Cytb_5[27] and house fly Cytb_5[28] (Figure 2b). An obvious difference between RvCytb_5 and other typical Cytb_5 proteins is a presence of a TS loop between β3 and β4. Although the TS loop does not form any secondary structures, the residues on it form a hydrogen bond network with each other and a salt bridge between Asp36 and Arg45 (Figure 2c). The TS loop shows few interactions with surrounding residues outside the TS loop, implying that it can flexibly move independent of other parts of the protein. One interaction is a hydrogen bond formed by the carbonyl O atom of Ser42 and the side chain of Arg35. The second one is a guanidino group stacking between Arg45 and Arg92. Such kind of arginine ion pairing is reported in several proteins and is thought to stabilize protein structures.[29]

As was expected from the spectroscopic data, hexa-coordinated b-type heme is observed in RvCytb_5. It is ligated by His56 and His80, which form hydrogen bonds with carbonyl O atoms of Gly59 and Phe75, respectively. The electron density map indicates that there are three different conformations of heme (Figure S1). The amino acid sequence alignment suggests that Trp18 and Tyr83 are potentially conserved residues among tardigrade Cytb_5-like proteins (Figure 1a). Trp18 is involved in interactions between N- and C-terminal regions, which are known to vary from Cytb_5 to Cytb_5.[28] The amide N atom of Trp18 forms a hydrogen bond with the side chain carboxylate group of Glu97 near the C-terminus (Figure S2a). Similar hydrogen bonds are observed in known Cytb_5 proteins although the positions of the residues having a carboxylate group are different from that in RvCytb_5 (Figure S2b,c). The N atom of the indole group in Trp18 interacts with the carbonyl O atom of Glu97 through a water molecule. The indole ring of Trp18 also shows a CH-π interaction with Ile21. Tyr83 on αE indirectly interacts with amino acid residues on the same helix (Figure S2a). Moreover, this bulky Tyr residue shows a van der Waals contact with one of the methyl carbon atoms in the heme. These interactions are not observed in typical Cytb_5 proteins (-Figure S2b,c). Figure 2e shows the electrostatic potential surface of RvCytb_5. In RvCytb_5, the surface surrounding the heme binding site and a cleft made by the TS loop are positively charged. Whereas, the typical Cytb_5 proteins show negatively charged surfaces around their heme binding sites (Figure 2f,g). While the surfaces of the typical Cytb_5 proteins have many residues that are negatively charged, RvCytb_5 displays positively charged residues (Figure 2h). Because the electrostatic potential surfaces of electron transfer proteins are usually optimized for their partner proteins to facilitate efficient ET complex formation, RvCytb_5 is thought to interact with proteins having negatively charged surfaces around their redox centers. That is, RvCytb_5 is probably involved in ET chains different from those related to typical Cytb_5 proteins. Considering that RvCytb_5 is a tardigrade-specific protein, it might be involved in biological processes unique to tardigrades. Identification of the partner protein(s) for RvCytb_5 is under way.
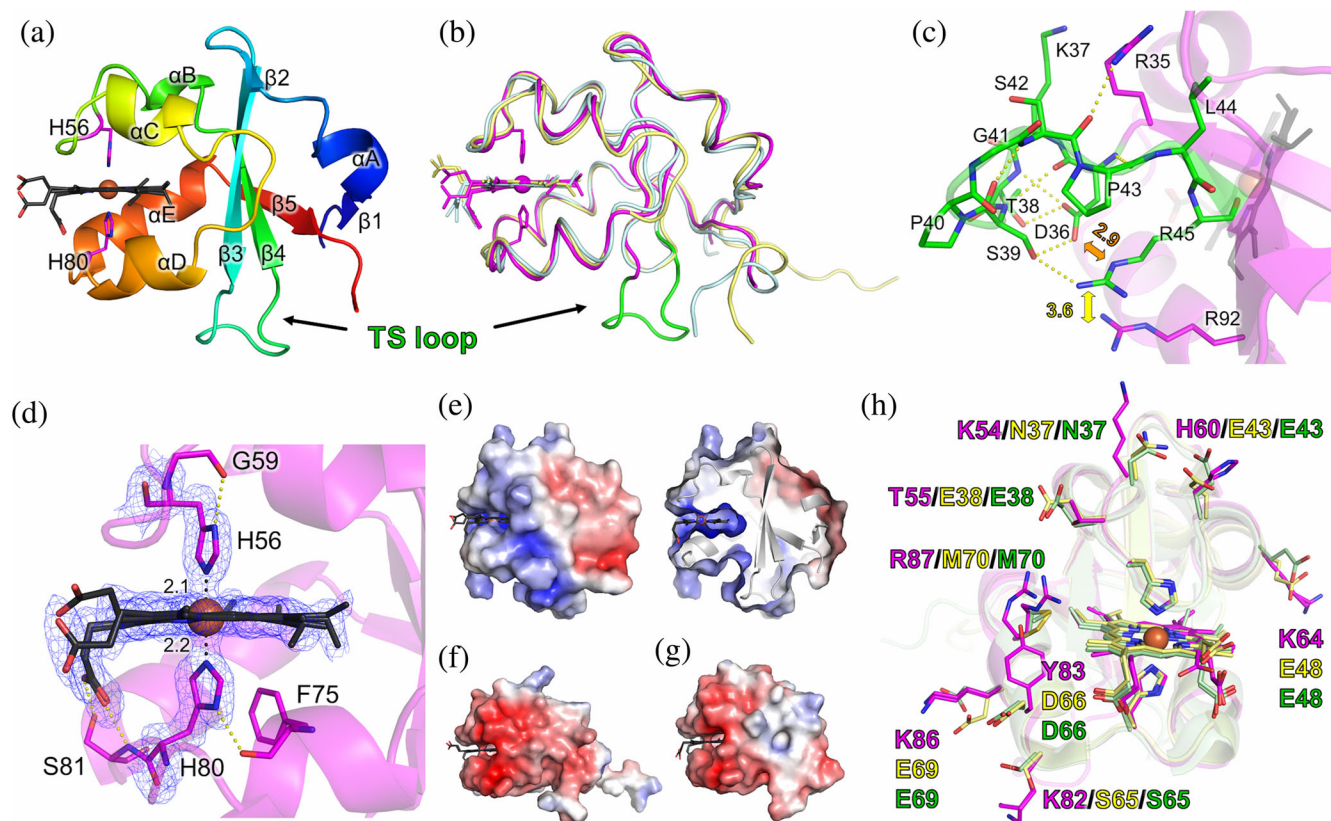
FIGURE 2 Structure of RvCytb_5. (a) Cartoon representation of the overall structure. Heme is illustrated by black sticks (carbon atoms) and a brown sphere (Fe atom). His ligands are colored by magenta. (b) Superposition of RvCytb_5 on human Cytb_5 (pale yellow: PDB code ID 3NER) and house fly Cytb_5 (pale green: PDB code ID 2IBJ). The TS loop is colored in green. (c) TS loop. Hydrogen bonds are shown by dotted yellow lines. A salt bridge is shown by orange double-headed arrows. Arginine stacking is shown by a yellow double-headed arrow. Distances are shown by Å unit. (d) Closeup view around the heme binding site with a sigma-A-weighted $2F_o–F_c$ map (1 σ: blue meshes). Hydrogen bonds and coordination bonds are shown by dotted yellow and black lines, respectively. Distances are shown by Å unit (e) Electrostatic potential surface of RvCytb_5 (left) and its cross-section view (right). The electrostatic potential is represented as a gradient from negative (red: $−5\ k_BT/e_c$) to positive (blue: $5\ k_BT/e_c$) (f) Electrostatic potential surface of human Cytb_5. (g) Electrostatic potential surface of house fly Cytb_5. (h) Comparison of residues contributing to electrostatic potential. Magenta: RvCytb_5; yellow: human Cytb_5; green: house fly Cytb_5

3 | MATERIALS AND METHODS

3.1 | Sequence alignment

Homology analyses were performed by BLAST.[30] Sequence alignment was performed by Clustal Omega[31] for structurally characterized Cytb_5 proteins and Cytb_5-like proteins showing the top five scores in the BLAST analysis. The alignment figure was generated by ESpript.[32] Phylogenetic analysis by a maximum likelihood method was conducted in MEGA X.[33]

3.2 | Protein expression and purification

The GenBank accession ID of the structural gene for RvCytb_5 from *R. varieornatus* is GAV03092.1. A synthesized and codon optimized DNA coding RvCytb_5(10–102)

was purchased from GenScript. The gene was cloned into a pET28a vector. A 6× His tag followed by a tobacco etch virus (TEV) protease site (ENLYFQS) was attached at the N-terminus of RvCytb_5(10–102) for purification. Its complete sequence is shown in Appendix S1 of Supporting Information. The protein was expressed in *Escherichia coli* BL21 Star(DE3) (Invitrogen, Waltham, MA). At culture optical density of ∼0.6, 0.5 mM isopropyl β-D-1 thiogalactopyranoside along with 0.5 mM aminolevulinic acid was added to induce expression. After 18 hr at 18°C, the bacterial pellet was collected and then sonicated in a buffer containing 20 mM Tris–HCl pH 8, 300 mM NaCl, benzonase (Merck Millipore, Burlington, MA), and a complete Protease Inhibitor Cocktail tablet (Roche, Basel, Basel-Stadt, Switzerland). The resulting solution was centrifuged and supernatant was purified using a HiTrap TALON column (GE healthcare, Chicago, IL). A buffer used to equilibrate the column and wash the sample

consisted of 20 mM Tris–HCl pH 8 and 5 mM imidazole. A buffer used for elution consisted of 20 mM Tris–HCl pH 8 and 200 mM imidazole. The sample was incubated with TEV protease and imidazole was removed through dialysis against 20 mM Tris–HCl pH 8 overnight at room temperature. The sample was then loaded on a HisTrap column (GE healthcare) equilibrated by 20 mM Tris–HCl pH 8 and 40 mM imidazole. The flow-through fraction was dialyzed against 50 mM Phosphate buffer pH 6.0 and purified by a HiTrap SP column (GE healthcare). The fractions containing RvCytb_5 were collected and further purified using a Hiload 16/60 Superdex 75 gel filtration column (GE healthcare). As for gel filtration, 20 mM Tris–HCl buffer pH 8 was used.

3.3 | Crystallization

Crystallization was performed by the sitting drop vapor-diffusion method. A crystallization machine mosquito (TTP LabTech, Melbourn, Hertfordshire, UK) was used to prepare drops on 96-well VIOLAMO plates (AS ONE, Osaka, Osaka, Japan). The reservoir solution was 60 µl, and 0.1 µl protein solution was mixed with 0.1 µl reservoir solution. After 4 months, a crystal appeared under the condition of 26 mg/ml RvCytb_5, 22% (w/v) polyethylene glycol 4000, and 50 mM 4-(2-hydroxyethyl)-1-piperazineethanesulfonic acid (HEPES) buffer pH 7.5 at 20°C. Before the crystal was frozen by liquid nitrogen, it was soaked in the crystallization solution supplemented by 15% v/v ethylene glycol.

3.4 | X-ray data collection, processing, structure solution, and refinement

X-ray diffraction experiment was performed on the BL44XU beamline of SPring-8, Hyogo, Japan. Diffraction images were collected at 100 K using an EIGER X 16 M detector (Dectris, Philadelphia, PA). A 0.8 mm Al attenuator was used to weaken X-ray. The crystal-to-detector distance was 160 mm. The exposure time per frame and the oscillation angle were 0.1 s and 0.1°, respectively. The dataset was processed using XDS[34] and scaled by Aimless.[35] Phase determination and initial model building was performed by CRANK2.[36] Manual model building was performed using Coot.[37] The program refmac5 in the ccp4 suite[38] and the program phenix.refine[39] were used for structural refinement. Anisotropic parameters were introduced because of its high resolution. The stereochemical quality of the final model was checked by Molprobity.[40] Data collection and refinement statistics

are summarized in Table 1. The coordinate and structure factor files are deposited at the Protein Data Bank (PDB code ID: 7BWH). Raw data is available at Integrated Resource for Reproducibility in Macromolecular Crystallography (https://proteindiffraction.org/).

3.5 | UV–visible absorption spectroscopy

The samples were in a 1 cm quartz cell. UV–visible absorption spectra of oxidized RvCytb_5 were recorded in 20 mM HEPES pH 7.1 with spectramax M2 and softmax pro 5.4 software (Molecular Devices, San Jose, CA) at room temperature. UV–vis spectrum of reduced RvCytb_5 in 20 mM HEPES pH 7.1 was recorded by adding 5 mM sodium dithionite at room temperature.

AUTHOR CONTRIBUTIONS
Yohta Fukuda: Conceptualization; data curation; formal analysis; funding acquisition; investigation; visualization; writing-original draft. **JeeEun Kim:** Data curation; formal analysis; investigation; writing-review and editing.

CONFLICT OF INTEREST
The authors declare no competing financial interests.

ORCID
Yohta Fukuda https://orcid.org/0000-0002-7386-8201

REFERENCES
1. Nelson DR. Current status of the Tardigrada: Evolution and ecology. Integrat Comparat Biol. 2002;42:652–659.
2. Keilin D. The problem of anabiosis or latent life: History and current concept. Proc Roy Soc Lond B. 1959;150:149–191.
3. Møbjerg N, Halberg KA, Jørgensen A, et al. Survival in extreme environments – On the current knowledge of adaptations in tardigrades. Acta Physiol. 2011;202:409–420.
4. Rahm PG. Biologische und physiologische Beiträge zur Kenntnis de Moosfauna Zeitschrift allgemeine. Physiologie. 1921;20:1–35.
5. Becquerel P. La suspension de la vie au dessus de 1/20 K absolu par demagnetization adiabatique de l'alun de fer dans le vide

les plus eléve. Compt Rend Hebdomad Séances de l'Acad Sci. 1950;231:261–263.

6. May RM, Maria M, Guimard MJ. Action différentielle des rayons x et ultraviolets sur le tardigrade Macrobiotus areolatus, a l'état actif et desséché. Bull Biol Fr Belg. 1964;98:349–367.

7. Horikawa DD, Sakashita T, Katagiri C, et al. Radiation tolerance in the tardigrade *Milnesium tardigradum*. Int J Radiat Biol. 2006;82:843–848.

8. Horikawa DD, Cumbers J, Sakakibara I, et al. Analysis of DNA repair and protection in the Tardigrade *Ramazzottius varieornatus* and *Hypsibius dujardini* after exposure to UVC radiation. PLoS One. 2013;8:e64793.

9. Horikawa DD, Yamaguchi A, Sakashita T, et al. Tolerance of anhydrobiotic eggs of the Tardigrade *Ramazzottius varieornatus* to extreme environments. Astrobiology. 2012;12: 283–289.

10. Utsugi K, Noda H. Vacuum tolerance of tardigrades. Proc NIPR Symp Polar Biol. 1995;8:202.

11. Ono F, Saigusa M, Uozumi T, et al. Effect of high hydrostatic pressure on to life of the tiny animal tardigrade. J Phys Chem Solid. 2008;69:2297–2300.

12. Seki K, Toyoshima M. Preserving tardigrades under pressure. Nature. 1998;395:853–854.

13. Ramløv H, Westh P. Cryptobiosis in the Eutardigrade Adorybiotus (Richtersius) coronifer: Tolerance to alcohols, temperature and de novo protein synthesis. Zoolog Anzeiger. 2001;240:517–523.

14. Horikawa DD, Kunieda T, Abe W, et al. Establishment of a rearing system of the extremotolerant tardigrade *Ramazzottius varieornatus*: A new model animal for astrobiology. Astrobiology. 2008;8:549–556.

15. Jönsson KI, Rabbow E, Schill RO, Harms-Ringdahl M, Rettberg P. Tardigrades survive exposure to space in low earth orbit. Curr Biol. 2008;18:R729–R731.

16. Fukuda Y, Miura Y, Mizohata E, Inoue T. Structural insights into a secretory abundant heat-soluble protein from an anhydrobiotic tardigrade, *Ramazzottius varieornatus*. FEBS Lett. 2017;591:2458–2469.

17. Fukuda Y, Inoue T. Crystal structure of secretory abundant heat soluble protein 4 from one of the toughest "water bears" micro-animals *Ramazzottius varieornatus*. Protein Sci. 2018;27: 993–999.

18. Kim J, Fukuda Y, Inoue T. Crystal structure of Kumaglobin: A hexacoordinated heme protein from an anhydrobiotic tardigrade, *Ramazzottius varieornatus*. FEBS J. 2019;286: 1287–1304.

19. Smith MA, Cross AR, Jones OTG, Griffiths WT, Stymne S, Stobart K. Electron-transport components of the 1-acyl-2-oleoyl-sn-glycero-3-phosphocholine Δ12-desaturase (Δ12-desaturase) in microsomal preparations from developing safflower (*Carthamus tinctorius* L.) cotyledons. Biochem J. 1990;272:23–29.

20. Fukushima H, Grinstead GF, Gaylor JL. Total enzymic synthesis of cholesterol from lanosterol. Cytochrome b5-dependence of 4-methyl sterol oxidase. J Biol Chem. 1981;256:4822–4826.

21. Hultquist DE, Passon PG. Catalysis of methaemoglobin reduction by erythrocyte cytochrome b5 and cytochrome b5 reductase. Nat New Biol. 1971;229:252–254.

22. Hashimoto T, Horikawa DD, Saito Y, Kuwahara H, Kozuka-Hata H, Shin-I T, Minakuchi Y, Ohishi K, Motoyama A, Aizu T,

Enomoto A, Kondo K, Tanaka S, Hara Y, Koshikawa S, Sagara H, Miura T, Yokobori SI, Miyagawa K, Suzuki Y, Kubo T, Oyama M, Kohara Y, Fujiyama A, Arakawa K, Katayama T, Toyoda A, Kunieda T (2016) Extremotolerant tardigrade genome and improved radiotolerance of human cultured cells by tardigrade-unique protein. Nat Commun 7: 12808.

23. Ozols J, Strittmatter P. Interaction of porphyrins and metalloporphyrins with apocytochrome b₅. J Biol Chem. 1964;239: 1018–1023.

24. Dewilde S, Kiger L, Burmester T, et al. Biochemical characterization and ligand binding properties of neuroglobin, a novel member of the globin family. J Biol Chem. 2001;276: 38949–38955.

25. Sawai H, Kawada N, Yoshizato K, Nakajima H, Aono S, Shiro Y. Characterization of the heme environmental structure of cytoglobin, a fourth globin in humans. Biochemistry. 2003; 42:5113–5142.

26. Smagghe BJ, Sarath G, Ross E, J-l H, Hargrove MS. Slow ligand binding kinetics dominate ferrous hexacoordinate hemoglobin reactivities and reveal differences between plants and other species. Biochemistry. 2006;45:561–570.

27. Parthasarathy S, Altuve A, Terzyan S, et al. Accommodating a non-conservative internal mutation by water-mediated hydrogen-bonding between beta-sheet strands: A comparison of human and rat type B (mitochondrial) cytochrome b₅. Biochemistry. 2011;50:5544–5554.

28. Wang L, Cowley AB, Terzyan S, Zhang X, Benson DR. Comparison of cytochromes b₅ from insects and vertebrates. Proteins. 2007;67:293–304.

29. Magalhaes A, Maigret B, Hoflack J, Gomes JNF, Scheraga HA. Contribution of unusual arginine-arginine short-range interactions to stabilization and recognition in proteins. J Protein Chem. 1994;13:195–215.

30. Altschul SF, Gish W, Miller W, Myers EW, Lipman DJ. Basic local alignment search tool. J Mol Biol. 1990;215:403–410.

31. Sievers F, Wilm A, Dineen D, et al. Fast, scalable generation of high-quality protein multiple sequence alignments using Clustal omega. Mol Syst Biol. 2011;7:539.

32. Robert X, Gouet P. Deciphering key features in protein structures with the new ENDscript server. Nucleic Acids Res. 2014; 42:W320–W324.

33. Kumar S, Stecher G, Li M, Knyaz C, Tamura K. MEGA X: Molecular evolutionary genetics analysis across computing platforms. Mol Biol Evol. 2018;35:1547–1549.

34. Kabsch W. XDS. Acta Crystallogr. 2010;D66(2):125–132.

35. Evans PR, Murshudov GN. How good are my data and what is the resolution? Acta Cryst. 2013;D69(7):1204–1214.

36. Skubak P, Pannu NS. Automatic protein structure solution from weak X-ray data. Nat Commun. 2013;4:2777.

37. Emsley P, Lohkamp B, Scott WG, Cowtan K. Features and development of coot. Acta Cryst. 2010;D66(4):486–501.

38. Murshudov GN, Skubak P, Lebedev AA, Pannu NS, Steiner RA, Nicholls RA, Winn MD, Long F, Vagin AA. REFMAC5 for the refinement of macromolecular crystal structures. Acta Cryst. 2011;D67(4):355–367.

39. Terwilliger TC, Zwart PH. PHENIX: A comprehensive python-based system for macromolecular structure solution. Acta Crystallogr. 2010;D66(2):213–221.

40. Chen VB, Arendall WB, 3rd Headd JJ, Keedy DA, Immormino RM, Kapral GJ, Murray LW, Richardson JS, Richardson DC. MolProbity: All-atom structure validation for macromolecular crystallography. Acta Cryst. 2010;D66(1):12–21.

SUPPORTING INFORMATION

Additional supporting information may be found online in the Supporting Information section at the end of this article.